MHD Toy Model of the Solar Radiative Zone

Céline Guervilly
advised by Pascale Garaud

January 12, 2009

1 Introduction

The Sun can be roughly divided into three different regions:

- The nuclear core, located in the inner part until 20% of the solar radius[1] where heat is produced by nuclear fusion of hydrogen.

- Between $0.2r_\odot$ and $0.7r_\odot$ the temperature is not high enough for nuclear reactions to proceed. The energy produced in the core is transported through this region by radiation which gives its name to this layer: the radiative zone. This layer is characterised by strong thermal stratification.

- In the outer region heat is transported primarily by convective motions. This leads to a well-mixed layer called the convective zone.

An important feature of the solar interior is its rotation profile. In this report, we describe a toy model of the solar radiative zone that can be used to investigate the interior rotation rate. During the last few decades, technological advances in helioseismology have provided accurate observations of the solar interior. The axisymmetric angular velocity profile deduced from observations is shown in figure 1. Differential rotation is observed within the convective zone: the equatorial region rotates about 30% faster than the polar regions. There, the rotation profile at a fixed radius can be fairly accurately expressed as

$$\Omega_{cz}(\theta) = \Omega_{eq}(1 - a\cos^2\theta - b\cos^4\theta), \tag{1}$$

where Ω_{eq} is the rotation rate at the equator and θ is the colatitude. The numbers a and b are determined by the observations. Near the lower region of the convective zone $a = 0.17$ and $b = 0.08$ (Schou *et al.* [4]). Meanwhile the radiative zone is near-uniformly rotating at a rate $\Omega_{rz} \simeq 0.93\Omega_{eq}$ where Ω_{eq} is the angular velocity at the equator at the bottom of the convective zone. The transition between the convective zone and the radiative zone is called the tachocline and has an important dynamical role.
An obvious question which comes to mind is why is the radiative zone rotating uniformly.
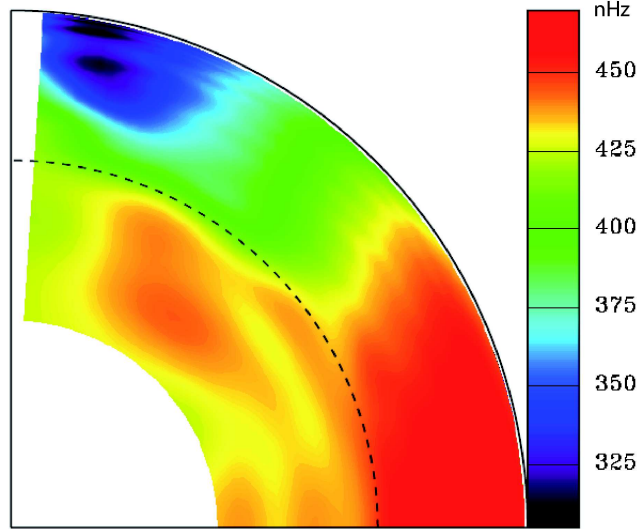
---

[1]Hereafter the solar radius is denoted $r_\odot$.

Figure 1: Angular velocity profile from solar observations in a meridional plane zonally and temporaly averaged. The outer layer is the convective zone and the inner layer is the radiative zone. The dashed line represents the base of the convection zone. Observations of the inner most regions are not available by helioseismology. Source: SOHO/MDI

A standard explanation for this feature assumes the presence of a primoridial magnetic field $\boldsymbol{B}$ confined within the radiative zone. Ferraro's isorotation law (1937), which is valid in the limit of negligible magnetic dissipation, states that

$$\boldsymbol{B} \cdot \nabla\Omega = 0, \tag{2}$$

for an axisymmetric rotating fluid in the steady state. Consequently the angular velocity is constant along magnetic field lines. If the field within the radiative zone has an "open" configuration, the magnetic field lines connected with the convective zone would transfer the differential rotation into the radiative zone; we shall call this a differentially rotating Ferraro state. On the otherhand, a close field configuration allows an uniformly rotating radiative zone. Gough and McIntyre [2] proposed a theoretical model (figure 2) that insured the uniform rotation of the radiative zone with:

- a differential rotation imposed by the convective zone,

- a primordial dipolar magnetic field in the radiative zone,

- down-welling meridional flows at the top of the radiative zone that confine the magnetic field, which itself prevents the flow from penetrating deeper into the radiative zone.

Numerical simulations based on this model have been carried out by Garaud & Garaud [1]. Their code is steady-state, axisymmetric, fully non-linear and models the bulk of the radiative zone as an anelastic conducting fluid. A radial velocity profile is imposed at the
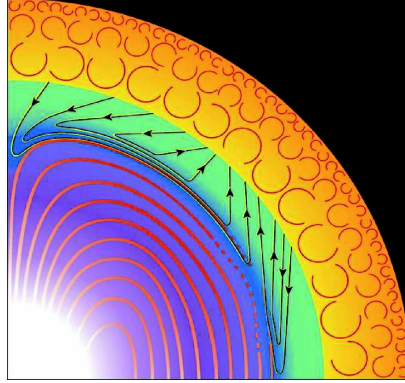
236

Figure 2: Picture of the model of Gough and McIntyre in a quadrant of the meridional plane. The red lines in the radiative zone (blue layer) represent the confined magnetic field, the black lines represent the meridional circulation which stays trapped in the top of the radiative zone. The yellow top layer is the convective zone.

top of the radiative zone and a no-slip condition is taken at the interface with the nuclear core. Both boundaries are assumed to be conducting with the same conductivity as the fluid. For low enough diffusivities they find that the rotation rate of the uniformly rotating region converges to about 86% of the imposed boundary rotation rate at the equator. The meridional circulation remains confined near the top of the radiative zone and deforms the poloidal magnetic field, which is almost confined within the radiative zone. When the inner core is assumed to be an electric insulator the equatorial region of the radiative zone rotates at 93% of the boundary rotation rate of the equator (figure 3, private communication). Following the work of Garaud & Garaud we will investigate the following questions:

- What is the effect of the convective zone dynamics on the radiative zone? How does the rotational shear propagate into the radiative zone?

- Can we build a simple analytical magnetohydrodynamic model of the radiative zone to predict the rotation rate of the interior?

- How does the rotation rate vary when we impose different magnetic boundary conditions?

2 Governing equations

A sketch of our toy model is presented in figure 4. The region we are interested in mimics the solar radiative zone: a conducting fluid fills the shell between a uniformly rotating inner sphere and a differentially rotating outer sphere. An axial dipolar magnetic field is imposed; we present here the case of an open magnetic field. We make the following assumptions:

- The system has reached a steady state.

- The fluid is incompressible, and density is constant in the whole volume.
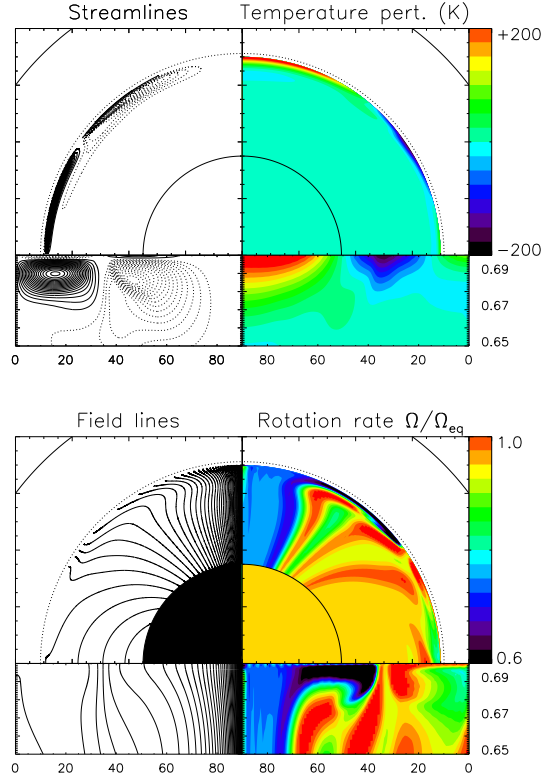
Figure 3: Results of a numerical simulation carried out with the code of Garaud & Garaud assuming an insulating inner core and a conducting outer boundary.

- In the solar radiative zone, the meridional circulation is slowed down by the strong stratification profile. Consequently, the angular momentum transported by the meridional flow is weak and will be neglected in this model. The non-linear terms are neglected.

- The imposed poloidal magnetic field is $\boldsymbol{B_p} = \nabla \times \left(\frac{A}{r \sin \theta} \hat{e}_\phi \right)$ with A the poloidal field potential $A(r, \theta) = B_0 r_{in}^3 \frac{\sin^2 \theta}{r}$ where B_0 is the imposed radial field at the poles on the inner sphere.

The magnetic field $\boldsymbol{B}$ and the velocity field $\boldsymbol{u}$ can therefore be decomposed in spherical coordinates as

$$\boldsymbol{B} = \left(\frac{1}{r^2 \sin \theta} \frac{\partial A}{\partial \theta}, -\frac{1}{r \sin \theta} \frac{\partial A}{\partial r}, B_\phi \right), \tag{3}$$
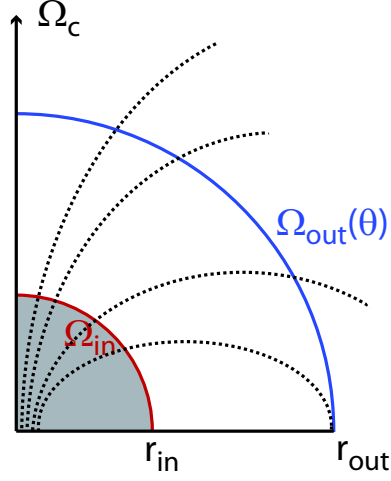
$$\boldsymbol{u} = (0, 0, r \sin \theta \Omega). \tag{4}$$

Figure 4: Diagram of our model.

The unknowns in our problem are the rotation rate Ω and the toroidal component of the magnetic field B_ϕ. The forms of Ω and B_ϕ are given by solving the azimuthal component of the Navier-Stokes equation and the magnetic induction equation respectively:

$$2\rho\boldsymbol{\Omega_c} \times \boldsymbol{u} = -\nabla p + \left(\frac{1}{\mu_0}\nabla \times \boldsymbol{B}\right) \times \boldsymbol{B} + \rho\nu\nabla^2\boldsymbol{u}, \tag{5}$$

$$0 = \nabla \times (\boldsymbol{u} \times \boldsymbol{B}) - \eta\nabla \times \nabla \times \boldsymbol{B}, \tag{6}$$

where ρ is the density, Ω_c the (constant) global rotation of the system, μ_0 the magnetic permeability, ν and η the viscous and the magnetic diffusivities respectively.

Rigid rotation is assumed at the interface with the inner sphere. Therefore, the angular velocity at the inner boundary is

$$\Omega(r_{in}, \theta) = \Omega_{in}. \tag{7}$$

At the outer boundary we use the angular velocity profile of the solar convective zone

$$\Omega(r_{out}, \theta) = \Omega_{out}(\theta) = \Omega_{eq}(1 - a\cos^2\theta - b\cos^4\theta). \tag{8}$$

For the toroidal magnetic field we will test different boundary conditions in order to evaluate their influence on the rotation profile. If we assume that the region exterior to the fluid is an electric insulator then the toroidal magnetic field has to be zero at the boundaries:

$$B_\phi(r_{in}, \theta) = 0, \tag{9}$$

$$B_\phi(r_{out}, \theta) = 0. \tag{10}$$

239

If we assume that the fluid is surrounded by a conductor with the same permeability and conductivity as the fluid in the shell, then the radial and tangential components of the magnetic field and its derivatives must be continuous, and the induction equation in a steady state provides us the following boundary condition:

$$[\nabla^2 \boldsymbol{B}]_\phi = 0 \quad \text{for} \quad r < r_{in} \quad \text{and} \quad r > r_{out}. \tag{11}$$

A difficult question is to decide which boundary condition is more relevant for the solar interior. This work will shed some light on the problem.

Finally the angular momentum must be conserved since the system is in a steady-state. Therefore the total torque applied in a spherical shell in the fluid is equal to zero:

$$\int_0^{\pi/2} \left(\rho \nu r^2 \sin^2 \theta \frac{\partial \Omega}{\partial r} + r \sin \theta \frac{B_r B_\phi}{\mu_0} \right) \sin \theta d\theta = 0. \tag{12}$$

The first term is the viscous torque whereas the second term is the magnetic torque. This equation determines uniquely Ω_{in}.

3 Insulating boundary conditions

We consider first the magnetic boundary conditions (9) and (10).

3.1 Solution in the bulk

In the bulk of the fluid, we will assume that we are in the limit of small magnetic and viscous diffusivities. This assumption is roughly valid in the Sun since the magnetic and viscous Ekman numbers $E_\eta^\odot$ and $E_\nu^\odot$ which measure the ratio of magnetic and viscous diffusivities (resp.) over the Coriolis force are assumed to be about 3×10^{-14} and 2×10^{-15} (resp.). We will therefore neglect both the viscous and magnetic diffusivities. Given our assumptions, the equilibria that govern the system are

$$2\rho \boldsymbol{\Omega_c} \times \boldsymbol{u} = -\nabla p + \left(\frac{1}{\mu_0} \nabla \times \boldsymbol{B} \right) \times \boldsymbol{B}, \tag{13}$$

$$0 = \nabla \times (\boldsymbol{u} \times \boldsymbol{B}). \tag{14}$$

Combining the ϕ-component of equation (14) and equation (4) and the fact that $\boldsymbol{u}$ and $\boldsymbol{B}$ are divergence-free, we obtain

$$[\nabla \times (\boldsymbol{u} \times \boldsymbol{B})]_\phi = r \sin \theta \boldsymbol{B_p} \cdot \nabla \Omega = 0. \tag{15}$$

Therefore in the bulk, the fluid is in a Ferraro iso-rotation state:

$$\boldsymbol{B_p} \cdot \nabla \Omega = 0, \tag{16}$$

or in other words Ω is constant along the poloidal magnetic field lines in a meridional plane. Using the ϕ-component of equation (13), we find

$$\left[\left(\frac{1}{\mu_0} \nabla \times \boldsymbol{B} \right) \times \boldsymbol{B} \right]_\phi = \frac{1}{r \sin \theta} \boldsymbol{B_p} \cdot \nabla (r \sin \theta B_\phi) = 0, \tag{17}$$

240

so the quantity $S \equiv r \sin \theta B_\phi$ is also constant along poloidal magnetic field lines.

Moreover, we can show that $\boldsymbol{B_p} \cdot \nabla A = 0$. Since $A(r, \theta) \propto \frac{\sin^2 \theta}{r}$ then $\frac{\sin^2 \theta}{r}$ remains constant along a magnetic field line. This determines the relationship between θ_{in} (the colatitude of emergence of a field line out of the core) and θ_{out} the colatitude where the same field line connects with the convection zone (figure 5):

$$\frac{\sin^2 \theta_{in}}{r_{in}} = \frac{\sin^2 \theta_{out}}{r_{out}} \ . \tag{18}$$

The relationship between θ_{out} and θ_{in} can be written as $\theta_{out} = \Theta(\theta_{in})$ where
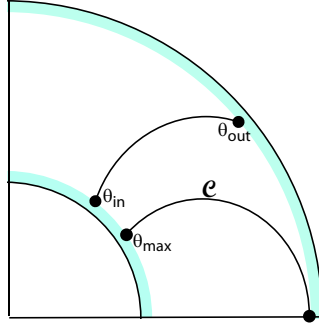

Figure 5: Picture of the dipolar magnetic field lines in the bulk of the fluid. The blue layers represent the boundary layers.

$$\Theta(\theta) = \sin^{-1}\left((r_{out}/r_{in})^{1/2} \sin \theta\right). \tag{19}$$

The magnetic field line which connects to the equatorial plane at r_{out}, which we call $\mathcal{C}$, crosses the inner sphere at the colatitude

$$\theta_{max} = \sin^{-1}\left(\frac{r_{in}}{r_{out}}\right)^{1/2} = \Theta\left(\frac{\pi}{2}\right). \tag{20}$$

The poloidal magnetic field lines which have a colatitude at the inner sphere between θ_{max} and $\pi/2$ connect to the inner sphere in the southern hemisphere without crossing the outer sphere. Because of isorotation we will assume that the equatorial region included between the equatorial plane and the line $\mathcal{C}$ is rotating uniformly. Consequently the integration of the total torque in r_{in} can be reduced to the region above the magnetic field line $\mathcal{C}$:

$$\int_0^{\pi/2} \longrightarrow \int_0^{\theta_{max}} \ . \tag{21}$$

This approximation allows us to avoid the equatorial region where the boundary layer approach presented in the next section is not valid.

3.2 Solution in the boundary layers

Equations (5) and (6) in the azimuthal direction can be written in spherical coordinates as (Rüdiger & Kitchatinov, [3])

$$\eta \left[\frac{\partial}{\partial \theta} \left(\frac{1}{\sin \theta} \frac{\partial (B_\phi \sin \theta)}{\partial \theta} \right) + r \frac{\partial^2 (B_\phi r)}{\partial r^2} \right] = r \left(\frac{\partial \Omega}{\partial \theta} \frac{\partial A}{\partial r} - \frac{\partial \Omega}{\partial r} \frac{\partial A}{\partial \theta} \right), \tag{22}$$

$$\rho \nu \left[\frac{1}{\sin^3 \theta} \frac{\partial}{\partial \theta} \left(\sin^3 \theta \frac{\partial \Omega}{\partial \theta} \right) + \frac{1}{r^2} \frac{\partial}{\partial r} \left(r^4 \frac{\partial \Omega}{\partial r} \right) \right] =$$
$$\frac{1}{\mu_0 r^2 \sin^3 \theta} \left(r \frac{\partial A}{\partial r} \frac{\partial (B_\phi \sin \theta)}{\partial \theta} - \sin \theta \frac{\partial A}{\partial \theta} \frac{\partial (B_\phi r)}{\partial r} \right). \tag{23}$$

First we will consider the inner boundary layer. In order to simplify these equations we will use a stretched variable in the boundary layer:

$$\zeta = \frac{r - r_{in}}{\delta_{in}}. \tag{24}$$

We assume that variations with θ are very small compared to those in the ζ-direction. We will therefore neglect the θ-derivative in the equations. Note that this hypothesis happens to fail near the equator where the boundary layer thickness diverges (see below). Equations (22) and (23) become

$$\eta \frac{r_{in}}{\delta_{in}} \frac{\partial^2 B_\phi}{\partial \zeta^2} = -\frac{\partial \Omega}{\partial \zeta} \frac{\partial A}{\partial \theta}, \tag{25}$$

$$\rho \nu \mu_0 \frac{r_{in}^3 \sin^2 \theta}{\delta_{in}} \frac{\partial^2 \Omega}{\partial^2 \zeta} = -\frac{\partial A}{\partial \theta} \frac{\partial B_\phi}{\partial \zeta}. \tag{26}$$

Combining these equations, we find

$$\frac{\partial^3 B_\phi}{\partial \zeta^3} = \frac{\partial B_\phi}{\partial \zeta}, \tag{27}$$

$$\frac{\partial^3 \Omega}{\partial \zeta^3} = \frac{\partial \Omega}{\partial \zeta}, \tag{28}$$

provided

$$\boxed{\delta_{in} = \frac{(\mu_0 \rho \nu \eta)^{1/2}}{2 \cos \theta B_0}.} \tag{29}$$

This boundary layer is an Hartmann layer. Its thickness is proportional to the geometric mean of the magnetic and viscous diffusivities. Moreover the layer becomes thinner if we increase the strength of the imposed magnetic field. The layer is singular near the equator where $\cos \theta \to 0$.

The solutions of (27) and (28) are

$$B_\phi(\zeta, \theta) = b_0^{in}(\theta) + b_1^{in}(\theta)e^\zeta + b_2^{in}(\theta)e^{-\zeta}, \tag{30}$$

$$\Omega(\zeta, \theta) = \Omega_0^{in}(\theta) + \Omega_1^{in}(\theta)e^\zeta + \Omega_2^{in}(\theta)e^{-\zeta}. \tag{31}$$

When $\zeta \to \infty$, Ω and B_ϕ have to remain bounded, and so $\Omega_1^{in} = b_1^{in} = 0$. Applying the boundary conditions and the matching conditions, we find

$$\Omega(\zeta \to 0, \theta) = \Omega_{in} = \Omega_0^{in}(\theta) + \Omega_2^{in}(\theta) , \tag{32}$$

$$\Omega(\zeta \to \infty, \theta) = \Omega_0^{in}(\theta) , \tag{33}$$

$$B_\phi(\zeta \to 0, \theta) = 0 = b_0^{in}(\theta) + b_2^{in}(\theta) , \tag{34}$$

$$B_\phi(\zeta \to \infty, \theta) = b_0^{in}(\theta) . \tag{35}$$

$\Omega_0^{in}(\theta)$ and $b_0^{in}(\theta)$ are the solutions in the bulk of the fluid where we neglect viscous and magnetic diffusivities. We will then call them $\Omega_0(r, \theta)$ and $b_0(r, \theta)$. Finally the solutions are

$$B_\phi(\zeta, \theta) = b_0(r_{in}, \theta)(1 - e^{-\zeta}), \tag{36}$$

$$\Omega(\zeta, \theta) = \Omega_0(r_{in}, \theta)(1 - e^{-\zeta}) + \Omega_{in} e^{-\zeta}. \tag{37}$$

Using either (25) or (26), we find the relation between b_0 and Ω_0:

$$b_0(\theta, r_{in}) = \frac{\delta_{in}}{\eta r_{in}} \frac{\partial A}{\partial \theta} \left(\Omega_0(r_{in}, \theta) - \Omega_{in} \right) = \left(\frac{\mu_0 \rho \nu}{\eta} \right)^{1/2} r_{in} \sin \theta \left(\Omega_0(r_{in}, \theta) - \Omega_{in} \right). \tag{38}$$

Since the boundary condition on the inner core imposed that $B_\phi(r_{in}, \theta) = 0$, and $\rho\nu$ is assumed to be constant in the boundary layer, (12) becomes

$$\int_0^{\theta_{max}} \sin^3 \theta \frac{\partial \Omega}{\partial r} d\theta = 0, \tag{39}$$

which can be written as

$$\int_0^{\theta_{max}} \frac{\sin^3 \theta}{\delta_{in}} \frac{\partial \Omega}{\partial \zeta} d\theta = 0. \tag{40}$$

Using (37), we have

$$\frac{\partial \Omega}{\partial \zeta} = \left(\Omega_0(r_{in}, \theta) - \Omega_{in} \right) e^{-\zeta} \implies \left. \frac{\partial \Omega}{\partial \zeta} \right|_{\zeta=0} = \Omega_0(r_{in}, \theta) - \Omega_{in}. \tag{41}$$

Moreover

$$\delta_{in} \propto \frac{1}{\cos \theta}. \tag{42}$$

Therefore (40) becomes

$$\int_0^{\theta_{max}} \sin^3 \theta \cos \theta \left(\Omega_0(r_{in}, \theta) - \Omega_{in} \right) d\theta = 0. \tag{43}$$

Condition (12) should be valid everywhere in the fluid. In the bulk of the fluid, the kinematic viscosity is neglected, so the torque applied to a spherical shell at radius $r_{in} + \epsilon$, where $\epsilon > \delta_{in}$, is only the magnetic torque and (12) becomes

$$\int_0^{\pi/2} (r_{in} + \epsilon) \sin^2 \theta \frac{B_r B_\phi(r_{in} + \epsilon, \theta)}{\mu_0} d\theta = 0. \tag{44}$$

243

Using the value of B_ϕ in the bulk given by (38) and since $B_r \propto \cos\theta$ we find the condition

$$\int_0^{\pi/2} \sin^3\theta \cos\theta \left(\Omega_0(r_{in} + \epsilon, \theta) - \Omega_{in}\right) d\theta = 0, \tag{45}$$

which is the same condition as previously. The viscous torque acts only on the boundary layer whereas the magnetic torque acts in the bulk, but together they maintain the previous condition everywhere in the fluid.

We have to determine the value of $\Omega_0(r_{in}, \theta)$ in order to calculate a value for Ω_{in}. To match $\Omega_0(r_{in}, \theta)$ to its value at the outer boundary we have to find the solution in the outer boundary.

We use the stretched variable in the outer boundary layer:

$$\xi = \frac{r_{out} - r}{\delta_{out}} . \tag{46}$$

Proceeding as for the inner boundary layer, we find

$$B_\phi(\xi, \theta) = b_0(r_{out}, \theta)(1 - e^{-\xi}), \tag{47}$$

$$\Omega(\xi, \theta) = \Omega_0(r_{out}, \theta)(1 - e^{-\xi}) + \Omega_{out}(\theta)e^{-\xi}, \tag{48}$$

with

$$b_0(r_{out}, \theta) = \left(\frac{\rho\nu\mu_0}{\eta}\right)^{1/2} r_{out} \sin\theta \left(\Omega_{out}(\theta) - \Omega_0(r_{out}, \theta)\right), \tag{49}$$

and

$$\delta_{out} = \frac{(\mu_0\rho\nu\eta)^{1/2}}{2\cos\theta B_0}\left(\frac{r_{out}}{r_{in}}\right)^3 = \delta_{in}\left(\frac{r_{out}}{r_{in}}\right)^3. \tag{50}$$

The thickness of the outer boundary layer δ_{out} is larger than that of the inner boundary because the imposed magnetic field is proportional to $1/r^3$, and therefore weaker at the outer boundary.

Since $S = B_\phi r \sin\theta$ is constant along a poloidal magnetic field line, we have

$$b_0(r_{in}, \theta_{in})r_{in} \sin\theta_{in} = b_0(r_{out}, \theta_{out})r_{out} \sin\theta_{out}. \tag{51}$$

Using (38) and (49), we find

$$(r_{in} \sin\theta)^2 \left(\Omega_0(r_{in}, \theta) - \Omega_{in}\right) = (r_{out} \sin\Theta(\theta))^2 \left(\Omega_{out}(\Theta(\theta)) - \Omega_0(r_{out}, \Theta(\theta))\right) . \tag{52}$$

Since the bulk of the fluid is in a state of iso-rotation, we expect that $\Omega_0(r_{in}, \theta) = \Omega_0(r_{out}, \Theta(\theta))$. Consequently,

$$\Omega_0(r_{in}, \theta) = \frac{1}{1 + \frac{(r_{in} \sin\theta)^2}{(r_{out} \sin\Theta(\theta))^2}}\Omega_{out}(\Theta(\theta)) + \frac{1}{1 + \frac{(r_{out} \sin\Theta(\theta))^2}{(r_{in} \sin\theta)^2}}\Omega_{in}, \tag{53}$$

$$\Omega_0(r_{in}, \theta) = \frac{1}{1 + \frac{r_{in}^3}{r_{out}^3}}\Omega_{out}(\Theta(\theta)) + \frac{1}{1 + \frac{r_{out}^3}{r_{in}^3}}\Omega_{in}. \tag{54}$$

244

The condition (43) becomes

$$\int_0^{\theta_{max}} \sin^3 \theta \cos \theta \left[\frac{1}{1 + \frac{r_{in}^3}{r_{out}^3}} \Omega_{out}(\theta_{out}) + \Omega_{in} \left(-1 + \frac{1}{1 + \frac{r_{out}^3}{r_{in}^3}} \right) \right] d\theta = 0, \qquad (55)$$

with

$$\Omega_{out}(\Theta(\theta)) = \Omega_{eq} \left[1 - a \left(1 - \frac{r_{in}}{r_{out}} \sin^2 \theta \right) - b \left(1 - \frac{r_{in}}{r_{out}} \sin^2 \theta \right)^2 \right]. \qquad (56)$$

We find

$$\frac{\Omega_{in}}{\Omega_{eq}} = \frac{\int_0^{\theta_{max}} \left(1 - a(1 - \frac{r_{in}}{r_{out}} \sin^2 \theta) - b(1 - \frac{r_{in}}{r_{out}} \sin^2 \theta)^2 \right) \sin^3 \theta \cos \theta d\theta}{\int_0^{\theta_{max}} \sin^3 \theta \cos \theta d\theta}, \qquad (57)$$

$$\frac{\Omega_{in}}{\Omega_{eq}} = 1 - \frac{a}{3} - \frac{b}{6}. \qquad (58)$$

Using the values provided by the observations of the Sun, $a = 0.17$ and $b = 0.08$, we find $\Omega_{in}/\Omega_{eq} = 0.93$. The remarks that we can draw from this result are:

- The result does not depend on the gap between the two spheres.

- It is the same value as that observed in the Sun. Therefore we can wonder if this value has a physical explanation. It is hard to answer this question but it is possible that our simple model catches an essential feature of the dynamics of the solar radiative zone.

3.3   No inner boundary

We wonder what happens if there is no inner boundary layer. Indeed the interface between the nuclear core and the radiative zone is not a physical barrier submitted to no-slip conditions. The nuclear core is defined simply as the place where the temperature is large enough to trigger nuclear reactions. Therefore the interface between the inner core and the radiative zone is merely an isotherm, and not a physical boundary.

The total torque applied on the outer sphere is

$$\int_0^{\pi/2} \rho \nu r_{out}^2 \sin^3 \theta \left. \frac{\partial \Omega}{\partial r} \right|_{r_{out}} d\theta = 0, \qquad (59)$$

$$\left. \frac{\partial \Omega}{\partial r} \right|_{r_{out}} = -\frac{1}{\delta_{out}} \left. \frac{\partial \Omega}{\partial \xi} \right|_{\xi \to 0} = -\frac{1}{\delta_{out}} (\Omega_0(r_{out}, \theta) - \Omega_{out}(\theta)). \qquad (60)$$

We will match the solution in the bulk at r_{out} with Ω_{in} the angular velocity at r_{in}. Under these assumption the whole radiative zone is rotating uniformly at the angular velocity Ω_{in} (see figure 6). Consequently we have

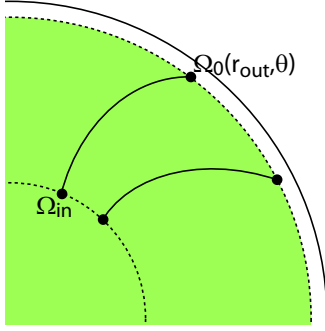$$\int_0^{\pi/2} \sin^3 \theta \cos \theta (\Omega_{out}(\theta) - \Omega_{in}) d\theta = 0, \qquad (61)$$

245

Figure 6: Diagram of the model when considering no inner boundary. The radiative zone is uniformly rotating and the outer boudary layer undergoes a strong shear.

where

$$\Omega_{out}(\theta) = \Omega_{eq} \left(1 - a \cos^2 \theta - b \cos^4 \theta \right). \tag{62}$$

The whole interior is rotating at the angular velocity

$$\frac{\Omega_{in}}{\Omega_{eq}} = \frac{\int_0^{\pi/2} \sin^3 \theta \cos \theta (1 - a \cos^2 \theta - b \cos^4 \theta) d\theta}{\int_0^{\pi/2} \sin^3 \theta \cos \theta d\theta}, \tag{63}$$

$$\frac{\Omega_{in}}{\Omega_{eq}} = 1 - \frac{a}{3} - \frac{b}{6}. \tag{64}$$

We find the same expression as previously. If a mechanism is able to impose an uniform rotation to the radiative zone interior, then the presence of the outer boundary alone prevents the transfer of the angular velocity from the convective zone to the deep radiative zone along open magnetic field lines. In the outer boundary layer the zonal shear is very strong, as in the solar tachocline.

3.4   Characteristic features of this toy model of the solar radiative zone

Our boundary layer analysis provided a solution valid from the poles to the magnetic field line $\mathcal{C}$. The solution in the equatorial zone can be deduced from geometrical considerations:

- The solutions are either symmetric or antisymmetric with respect to the equatorial plane due to the symmetry of the imposed poloidal magnetic field. The angular velocity, for example, is symmetric.

- The toroidal field on the other hand is antisymmetric with respect to the equatorial plane; therefore S is also antisymmetric. An important consequence of this fact is that since S has to be constant along the magnetic field lines, S and so the toroidal field must be equal to zero in the equatorial region where field lines connect the northern and southern hemispheres.

246

- Another consequence is that the equatorial region, defined as the region between the equatorial plane and the magnetic field line $\mathcal{C}$, rotates at the constant angular velocity $\Omega_{in} = 0.93\Omega_{eq}$.

- The presence of a rapidly rotating layer around the equatorial region is due to the fact that a magnetic field line that connects just above the equator in the outer sphere transfers the fast angular velocity of the convective zone at the equator until the inner sphere.

- This rapidly rotating layer shears the poloidal magnetic field lines and creates a strong toroidal magnetic field (the Ω-effect).

- Towards the poles the angular velocity transfered from the convective zone is lower. Therefore the angular velocity in the bulk decreases at high latitudes.

An outline of the geometry of our asymptotic model of the solar radiative zone is presented figure 7.
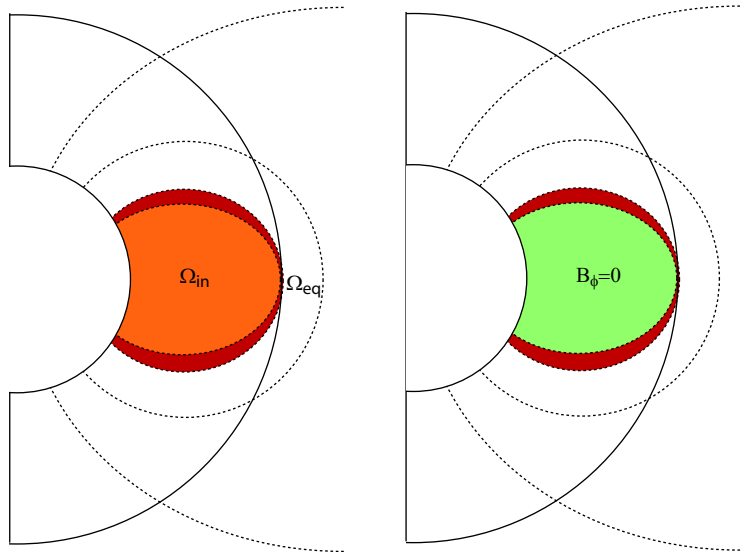

Figure 7: Asymptotic model of the conducting fluid flow between two rotating spheres (no viscosity, no magnetic diffusivity)

3.5 Comparison with numerical results

The code used to compare the analytical results with numerical simulations is a stripped version of the code of Garaud & Garaud [1] modified to solve equations (22) and (23) only. The same assumptions as in our analytical model are made except that the kinematic and

magnetic diffusivities are not neglected in the main body of the fluid. The same boundary conditions are adopted. Numerical simulations are limited by the fact that assuming very low diffusivities means that the boundary layers are very thin and can not be resolved numerically. To overcome this problem, diffusivities are enhanced by multiplying them by a factor f. $f = 1$ means that the values adopted in the simulations are the solar values. Figure 8 show the convergence of the numerical value of the ratio Ω_{in}/Ω_{eq} towards the analytical value of 0.93 when decreasing the factor f. The results of a numerical simulation are presented in figure 9. The structure of the angular velocity and the toroidal magnetic field are similar to the ones predicted by our model in section 3.4. The rapidly rotating layer is visible.
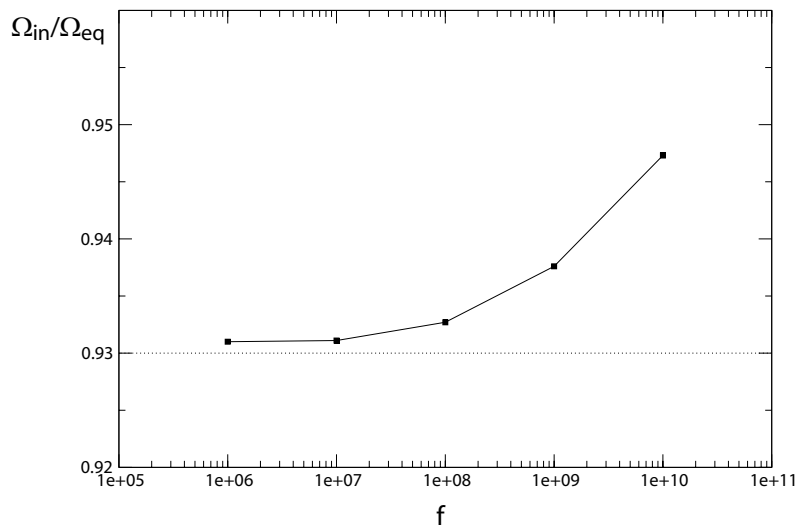

Figure 8: Ratio of the angular velocity at the inner sphere and at the equator of the convective zone in function of the factor f. The dots represent the results of the numerical simulations and the dashed line the analytical value. Note theat $f = 10^{10}$ corresponds to $E_\nu = 2 \cdot 10^{-5}$ and $E_\eta = 3 \cdot 10^{-4}$.

The total torque (12) computed numerically as a function of the colatitude (figure 10) is equal to zero if $\theta > \theta_{max}$. This remark validates our assumption of neglecting the contribution of the equatorial region (section 3.1).

4   Conducting boundary conditions

We now consider applying boundary condition (11) to the toroidal magnetic field. In the convective zone and inner core the media are assumed to have the same electic conductivity and permeability as the fluid in the shell. Therefore the tangential components of the magnetic field are continuous. Outside the fluid domain B_ϕ satisfies the induction equation
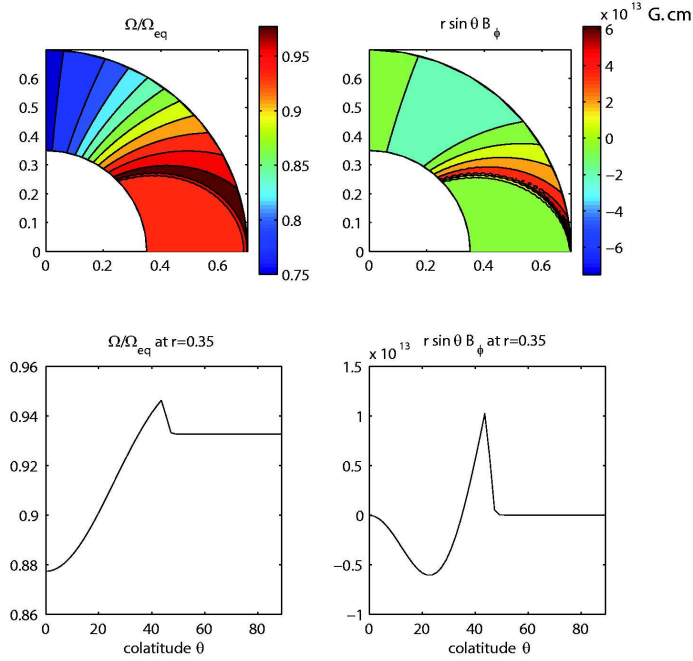
Figure 9: Results of the numerical simulations computed at $f = 10^8$. Left: angular velocity in a quadrant of the meridional plane (top) and at a fixed radius just above the inner boundary layer (bottom). Right: function $S = r \sin \theta B_\phi$ similarly plotted.
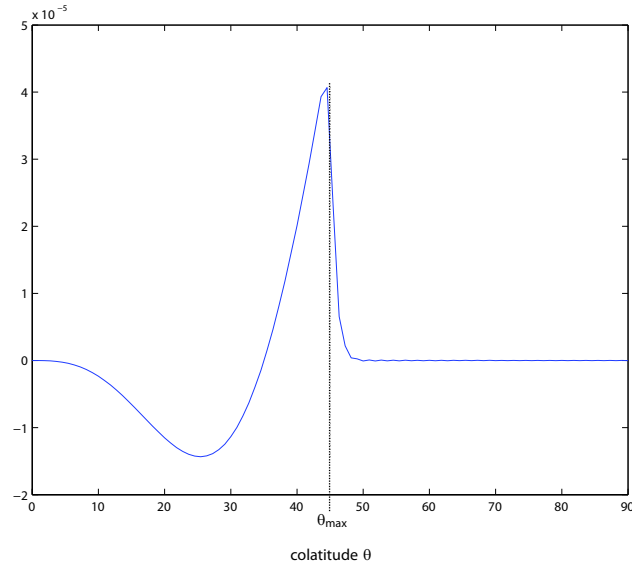

Figure 10: Total torque at r_{in} in function of the colatitude.

in the steady-state:

$$\left[\nabla^2 \boldsymbol{B}\right]_\phi = 0 \tag{65}$$

$$\Rightarrow \quad \nabla^2 B_\phi - \frac{B_\phi}{r^2 \sin^2 \theta} = 0. \tag{66}$$

The solution of this equation on both sides of the cavity are

$$B_\phi(r \le r_{in}, \theta) = \sum_{n=0}^\infty a_n^{in} r^n \frac{d}{d\theta}\left[P_n(\cos\theta)\right], \tag{67}$$

$$B_\phi(r \ge r_{out}, \theta) = \sum_{n=0}^\infty a_n^{out} r^{-(n+1)} \frac{d}{d\theta}\left[P_n(\cos\theta)\right], \tag{68}$$

where P_n is the n-th Legendre polynomial. The continuity of B_ϕ and its r-derivative has to be verified across the interface. Applying these conditions to the solutions in the boundary layers (30), we find

$$\sum_{n=0}^\infty a_n^{in} r_{in}^n \frac{d}{d\theta}\left[P_n(\cos\theta)\right] = b_0(r_{in}, \theta) + b_2^{in}(\theta), \tag{69}$$

$$\sum_{n=0}^\infty a_n^{in} n r_{in}^{n-1} \frac{d}{d\theta}\left[P_n(\cos\theta)\right] = -\frac{1}{\delta_{in}} b_2^{in}(\theta), \tag{70}$$

$$\sum_{n=0}^\infty a_n^{out} r_{out}^{-(n+1)} \frac{d}{d\theta}\left[P_n(\cos\theta)\right] = b_0(r_{out}, \theta) + b_2^{out}(\theta), \tag{71}$$

$$\sum_{n=0}^\infty -a_n^{out}(n+1) r_{out}^{-(n+2)} \frac{d}{d\theta}\left[P_n(\cos\theta)\right] = \frac{1}{\delta_{out}} b_2^{out}(\theta). \tag{72}$$

The system of equations arising from this choice of boundary conditions is too complex to solve in spherical coordinates. For simplicity, we adopt a local cartesian box model for the boundary layers.

4.1 The Cartesian box

The model is illustrated in figure 11. We make the same assumptions as previously and introduce periodicity in the y-direction (equivalent to the θ-direction in spherical coordinates). The system is invariant in the x-direction, which corresponds to the ϕ-direction in the original spherical coordinates. A magnetic field is imposed in the z-direction, and depends only on y. The magnetic field and the velocity are decomposed in cartesian coordinates as

$$\boldsymbol{B} = (b, 0, B_0), \tag{73}$$

$$\boldsymbol{u} = (u, 0, 0). \tag{74}$$

We solve the system for the unknown b and u. The Navier-Stokes and the induction equations in the x-direction become under our assumptions

$$B_0(y)\frac{\partial b}{\partial z} = -\rho\nu\mu_0\nabla^2 u, \tag{75}$$

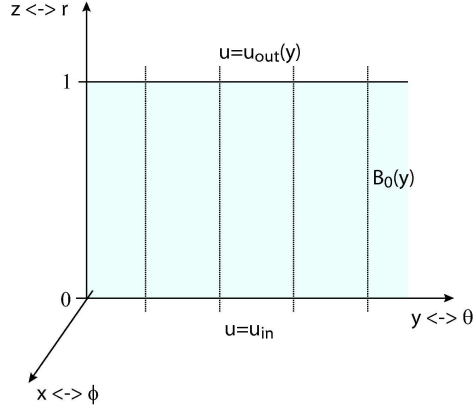$$B_0(y)\frac{\partial u}{\partial z} = -\eta\nabla^2 b. \tag{76}$$

Figure 11: Diagram of the cartesian box.

4.2 Boundary layers

As in the spherical case, we use a stretched variable in the boundary layers. For the inner boundary, we use

$$\zeta = \frac{z}{\delta_{in}}, \tag{77}$$

and for the outer boundary

$$\xi = \frac{1-z}{\delta_{out}}. \tag{78}$$

In our boundary layer approximation, the y-derivative will be neglected. The previous equations become in the inner boundary

$$B_0(y)\frac{\partial b}{\partial \zeta} = -\frac{\rho\nu\mu_0}{\delta_{in}}\frac{\partial^2 u}{\partial \zeta^2}, \tag{79}$$

$$B_0(y)\frac{\partial u}{\partial \zeta} = -\frac{\eta}{\delta_{in}}\frac{\partial^2 u}{\partial \zeta^2}. \tag{80}$$

In the outer boundary layer the equations are similar apart from the sign. Combining the above equations in each boundary layer, we find

$$\frac{\partial^3 b}{\partial \zeta^3} = \frac{\partial b}{\partial \zeta}, \tag{81}$$

$$\frac{\partial^3 u}{\partial \zeta^3} = \frac{\partial u}{\partial \zeta}, \tag{82}$$

with

$$\delta_{in} = \delta_{out} = \frac{(\rho\nu\eta\mu_0)^{1/2}}{B_0(y)} = \delta. \tag{83}$$

251

As previously, these boundary layers are Hartmann layers. The solutions of these equations are, in the inner boundary,

$$u(\zeta, y) = u_0(z = 0, y) + u_2^{in}(y)e^{-\zeta}, \tag{84}$$

$$b(\zeta, y) = b_0(z = 0, y) + b_2^{in}(y)e^{-\zeta}, \tag{85}$$

$$b_2^{in}(y) = \frac{\rho \nu \eta}{\delta B_0(y)} u_2^{in}(y). \tag{86}$$

The solutions in the outer boundary are analogous, apart from sign changes. Angular momentum conservation gives us the condition

$$\int_0^{2\pi} \left[\rho \nu \frac{\partial u}{\partial z} + \frac{1}{\mu_0} B_0 b \right] dy = 0. \tag{87}$$

Moreover, continuity of the velocity in the bulk along the magnetic field lines[2] of B_0 provides another condition

$$u_0(z = 1, y) = u_0(z = 0, y), \tag{88}$$

$$b_0(z = 1, y) = b_0(z = 0, y). \tag{89}$$

The boundary conditions on the velocity are

$$u(z = 0, y) = u_{in}, \tag{90}$$

$$u(z = 1, y) = u_{out}(y). \tag{91}$$

In order to find an analogy with the previous case, we will first study the case where $b = 0$ outside on both sides.

4.3   Insulating boundaries

In this case, the boundary conditions for the tangential magnetic field are

$$b(z = 0, y) = b_0(z = 0, y) + b_2^{in}(y) = 0, \tag{92}$$

$$b(z = 1, y) = b_0(z = 1, y) + b_2^{out}(y) = 0. \tag{93}$$

Using (86), we find

$$2b_0(z, y) = -b_2^{in} - b_2^{out} = \frac{\rho \nu \eta}{\delta B_0(y)} \left(u_2^{out}(y) - u_2^{in}(y) \right). \tag{94}$$

When $\zeta \to 0$ and $\xi \to 0$,

$$u_0(z = 0, y) + u_2^{in}(y) = u_{in}, \tag{95}$$

$$u_0(z = 0, y) + u_2^{out}(y) = u_{out}(y), \tag{96}$$

and using the continuity of u_0 in the bulk along the y-lines

$$u_2^{in}(y) - u_2^{out}(y) = u_{in} - u_{out}(y). \tag{97}$$

Plugging this equation into (87) we find

$$\int_0^{2\pi} B_0(y)(u_{out}(y) - u_{in})dy = 0. \tag{98}$$

This equation is analogous to (43) by geometrical transformation.

---

[2]lines of constant y.

4.4 Conducting boudaries

When conducting boundaries are applied, the tangential component of the field is continuous across the interface. Outside of the fluid, the tangential magnetic field satisfies

$$\frac{\partial^2 b}{\partial y^2} + \frac{\partial^2 b}{\partial z^2} = 0. \tag{99}$$

For $z \notin [0,1]$ the field can be written as

$$b(z \leq 0, y) = \beta_0^{in} + \sum_{n=1}^{\infty} \beta_n^{in}(z) e^{iny}, \tag{100}$$

$$b(z \geq 1, y) = \beta_0^{out} + \sum_{n=1}^{\infty} \beta_n^{out}(z) e^{iny}, \tag{101}$$

where the functions β_n satisfies

$$-n^2 \beta_n + \frac{\partial^2 \beta_n}{\partial z^2} = 0. \tag{102}$$

The solution of this equation is

$$\beta_n(z) = \alpha_n e^{\pm nz}, \tag{103}$$

which has to remain bounded

$$\text{if } z > 1: \quad \beta_n^{out}(z) = \alpha_n^{out} e^{-nz}, \tag{104}$$

$$\text{if } z < 0: \quad \beta_n^{in}(z) = \alpha_n^{in} e^{nz}. \tag{105}$$

The field is continuous at the interface so

$$b_0^{in}(y) + b_2^{in}(y) = \beta_0^{in} + \sum \beta_n^{in}(z=0) e^{iny}, \tag{106}$$

$$b_0^{out}(y) + b_2^{out}(y) = \beta_0^{out} + \sum \beta_n^{out}(z=1) e^{iny}. \tag{107}$$

The z-derivative of b also has to be continous across the interface which yields the two additional equations

$$-\frac{1}{\delta} b_2^{in}(y) = \sum_{n=1}^{\infty} n \beta_n^{in}(z=0) e^{iny}, \tag{108}$$

$$\frac{1}{\delta} b_2^{out}(y) = \sum_{n=1}^{\infty} -n \beta_n^{out}(z=1) e^{iny}. \tag{109}$$

Adding the previous equations yields

$$\frac{1}{\delta} \left(b_2^{in}(y) + b_2^{out}(y) \right) = -\sum_{n=1}^{\infty} n \left(\beta_n^{in}(z=0) + \beta_n^{out}(z=1) \right) e^{iny}. \tag{110}$$

253

Combining the relation between b_2 and u_2 in both boundary layers (86), we find

$$b_2^{in}(y) + b_2^{out}(y) = \frac{\rho\eta\nu}{B_0(y)}\frac{1}{\delta}(u_2^{in} - u_2^{out}), \tag{111}$$

$$b_2^{in}(y) + b_2^{out}(y) = \frac{\rho\eta\nu}{B_0(y)}\frac{1}{\delta}(u_{in} - u_{out}(y)). \tag{112}$$

The results of the previous equations gives us

$$\frac{\rho\eta\nu}{B_0(y)}\frac{1}{\delta^2}(u_{in} - u_{out}(y)) = -\sum_{n=1}^{\infty} n\left(\beta_n^{in}(z=0) + \beta_n^{out}(z=1)\right)e^{iny} \tag{113}$$

$$\Rightarrow \quad \int_0^{2\pi} \frac{\rho\eta\nu}{B_0(y)}\frac{1}{\delta^2}(u_{in} - u_{out}(y))dy =$$

$$-\int_0^{2\pi} \sum_{n=1}^{\infty} n\left(\beta_n^{in}(z=0) + \beta_n^{out}(z=1)\right)e^{iny}dy. \tag{114}$$

Since the box is 2π periodic in the y-direction and $\beta_n^{in}(z=0)$ and $\beta_n^{out}(z=1)$ are constant, the right-hand side is equal to zero. Since $\delta \propto 1/B_0$ we have

$$\int_0^{2\pi} B_0(y)(u_{out}(y) - u_{in})dy = 0. \tag{115}$$

This condition is similar to the case where $b = 0$ outside. Therefore we expect to find the same rotation rate in the radiative zone with this kind of boundary condition. This means that the boundary conditions imposed on the tangential field should *a priori* not influence the rotation rate of the fluid.
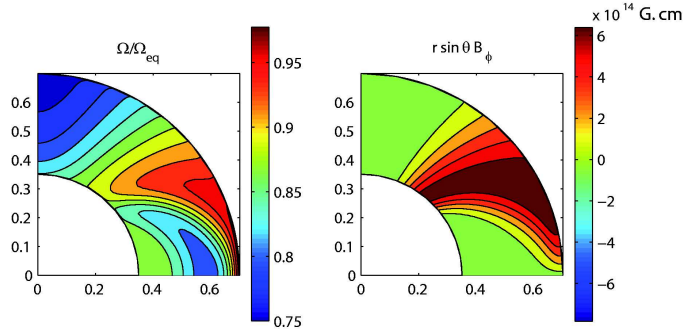
4.5   Numerical results

Figure 12: Numerical results with conducting boundary conditions.

The results of a simulation where $\left[\nabla^2 B\right]_\phi = 0$ is imposed on both sides is presented in figure 12. We find that the inner core rotates with angular velocity $\Omega_{in} = 0.86\Omega_{eq}$, contradicting the results of our analytic model of section 4.4. This value is lower than

254

the case with insulating boundaries because we notice that the fast angular velocity of the bottom of the equatorial convective zone is not propagated until the inner region of the radiative zone. We observe that the toroidal field B_ϕ is about ten times stronger than in the case where $B_\phi = 0$ was imposed on both boundaries. We also observe, in figure 12, that the Ferraro state is broken in the bulk of the fluid:

$$\boldsymbol{B_p} \cdot \nabla\Omega = \eta\nabla^2 B_\phi \neq 0. \tag{116}$$

It therefore appears that magnetic diffusivity plays a role in the bulk of the fluid which explains why our analytical model fails to reproduce the numerical results.

5 Conclusions

This work allows us to draw several conclusions and perspectives:

- Our toy model with an open magnetic field and vaccum magnetic boundary conditions provides a prediction of the interior rotation rate of the radiative zone in good agreement with both solar observations and full numerical simulations (including meridional circulations and all the non-linear terms (figure 3)). We find the solar value whereas the structure is not uniformly rotating. Moreover it allows us to understand the force balance of the system. The interior rotation rate of our simple model can provide insight into the physical processes that occur in the solar radiative zone.

- The boundary conditions chosen for the toroidal field have important consequences for the rotation of the fluid. However, the more relevant conditions for the Sun are difficult to determine.

- The confined field case needs to be investigated because of its believed relevance to the Sun.

References

[1] P. GARAUD AND J.-D. D. GARAUD, *Dynamics of the solar tachocline II: the stratified case*, ArXiv e-prints, 806 (2008).

[2] D. GOUGH AND M. E. MCINTYRE, *Inevitability of a magnetic field in the Sun's radiative interior*, Nature, 394 (1998), pp. 755–757.

[3] G. RUDIGER AND L. L. KITCHATINOV, *The slender solar tachocline: a magnetic model*, Astronomische Nachrichten, 318 (1997), pp. 273–279.

[4] J. SCHOU, H. M. ANTIA, S. BASU, R. S. BOGART, R. I. BUSH, S. M. CHITRE, J. CHRISTENSEN-DALSGAARD, M. P. DI MAURO, W. A. DZIEMBOWSKI, A. EFF-DARWICH, D. O. GOUGH, D. A. HABER, J. T. HOEKSEMA, R. HOWE, S. G. KORZENNIK, A. G. KOSOVICHEV, R. M. LARSEN, F. P. PIJPERS, P. H. SCHERRER, T. SEKII, T. D. TARBELL, A. M. TITLE, M. J. THOMPSON, AND J. TOOMRE, *Helioseismic Studies of Differential Rotation in the Solar Envelope by the Solar Oscillations Investigation Using the Michelson Doppler Imager*, The Astrophysical Journal, 505 (1998), pp. 390–417.